Plant macrofossil and biomarker evidence of fen-bog transition and associated changes in vegetation

Tiina Ronkainen [a*], Erin L. McClymont [b], Eeva-Stiina Tuittila [c,d], MinnaVäliranta [a]

[a] *Environmental Change Research Unit (ECRU), Department of Environmental Sciences, PO Box 65, FI-00014 University of Helsinki, Finland*

[b] *Department of Geography, Durham University. South Road, Durham DH1 3LE, UK*

[c] *Current address: School of Forest Sciences, University of Eastern Finland, PO Box 111, 80101 Joensuu, Finland*

[d] *Peatland Ecology Group, Department of Forest Sciences, PO Box 27, FI-00014 University of Helsinki, Finland*

[*] Corresponding author. *E mail address*: tiina.m.ronkainen@helsinki.fi (Tiina Ronkainen)

1. Introduction

Peatlands can be divided into two main types; fens and bogs, with the main factor controlling the peatland type and the occurrence of species being the ecohydrology, i.e., the quantity and quality of water (Wheeler and Proctor, 2000; Økland et al., 2001). Fens are relatively shallow and they receive water and nutrients from the underlying and surrounding mineral soils, groundwater and atmosphere (Rydin et al., 2006). **Various** sedge species, forbs, minerotrophic Sphagna (e.g. *Sphagnum subsecundum* and *S. riparium*) as well as brown mosses such as *Warnstorfia* species **dominate fen habitats**. In contrast, due to effective peat formation and the consequential increase in **height**of the peat surface, bogs are nutrient poor as they receive water and nutrients only through precipitation, maintaining plants**,** including

hummock Sphagna (e.g. *Sphagnum fuscum*), dwarf shrubs, lichens and true mosses (e.g. *Pleurozium schreberi* and *Polytrichum* spp.) (Rydin et al., 2006). **The** different environmental conditions in terms of the level of acidity, nutrient status and water table level means **that raised bog peats in boreal region** usually contain less-humified peat, while in groundwater-fed less acidic fen environments biomass decay is much faster and highly humified peat layers are formed (Moore et al., 2007).

Peatlands play an important role in atmospheric carbon cycling. Northern peatlands alone are estimated to store 547 (473-621) Pg organic carbon (Yu et al., 2010), yet, simultaneously peatlands are a natural source of CH_4 to the atmosphere (Matthews, 2000). As different peatland habitats and their vegetation, even within one peatland complex, have a vital role **in** the carbon budget of the peatland (e.g. Riutta et al., 2007), and the fact that bryophyte- and vascular plant- dominated communities differ in their CO_2 and CH_4 dynamics (Laine et al., 2007; Levy et al., 2012), it is important to be able to separate different habitats when reconstructing peatland dynamics back in time (Yu et al., 2013). Historical peatland habitats are preserved in peat layers as decomposed plant remains that form a key proxy when reconstructing the carbon budget of the peatland or historical climatic conditions (e.g. Barber et al.; 1998; Mauquoy et al.; 2002; Tuittila et al., 2007; Väliranta et al., 2007). Due to natural peatland succession **towards ombrotrophic conditions driven by peat height growth, minerotrophic (Frolking et al. 2010) fen peat layers are likely deposited under most of the** southern boreal raised bogs. Moreover, most of the high latitude peatlands are still the fen type of peatlands (e.g. Turunen et al., 2002) and in these environments the lack of identifiable plant remains may hamper palaeoecological and -climatological reconstructions.

Recently organic geochemistry analyses have shown that the lipid fractions of plants contain biomarkers for identifying different plant species and plant groups from peat archives.

48 Studies on bog peat environments have shown that plant group-specific chemical compounds
49 can be applied to identify fossil plants or plant groups from peat (e.g. Avsejs et al., 2002;
50 Bingham et al., 2010; Jia et al., 2008; McClymont et al., 2008; Xie et al., 2000). The most
51 widely analyzed compounds have been the *n*-alkanes: for instance, the difference between
52 concentrations of mid chain length (*n*-C_{23} and *n*-C_{25}) and long chain length (*n*-C_{29} and *n*-C_{33})
53 *n*-alkanes have been used to separate contributions of *Sphagnum* and vascular plant species in
54 the peat (e.g. Andersson et al., 2011; López-Días et al., 2010; Nichols et al., 2006; Ortiz et al.,
55 2011; Pancost et al., 2002; Ronkainen et al. 2013; Vonk and Gustafsson, 2009). Furthermore,
56 the *n*-C_{23}/*n*-C_{25} alkane ratio has been successfully used in tracking changes in *Sphagnum*
57 *fuscum* abundance in a peat section from Finland (Bingham et al., 2010).
58 Thus far, in environmental reconstructions the biomarker analyses have focused on bog peats
59 and plants typical to bogs. However, a pertinent question remaining is whether such plant-
60 specific biomarkers could also provide information about the past plant assemblages in fen
61 environments characterized by highly humified peat, where macrofossil remains are heavily
62 degraded and thus essential information for environmental reconstruction is lost. Some
63 previous studies have applied "bog" biomarker analyses throughout the peat profile,
64 including the fen peat section underlying the bog peat section (e.g. Andersson and Myers
65 2012; Andersson et al., 2011). However, our recent study of the *n*-alkane concentrations, *n*-
66 alkane ratios, and sterol distributions of moss and vascular plant species typical to fen
67 habitats **showed** differences between some of the biomarker distributions between plant
68 species characteristics to bogs and fens (Ronkainen et al., 2013). **As in** previous studies on
69 bog plants (Baas et al., 2000; Ficken et al., 1998; Nichols et al., 2006; Pancost et al., 2002)
70 fen *Sphagnum* species were also dominated by mid-chain *n*-alkanes and the above ground
71 parts of fen vascular plants by long-chain *n*-alkanes. However, results showed similarity in
72 the dominating *n*-alkanes of *Sphagnum* species and below-ground parts of sedges in studied

fen plants and thus, applying *n*-alkane ratios from bog plants to fen peats could result in incorrect interpretations about the actual proportions of these plant groups in peat (Ronkainen et al., 2013). Similar mid-chain *n*-alkane distributions in vascular plant roots were also reported by Huang et al. (2011). The similarity of *n*-alkane distributions in *Sphagnum* species and vascular plant below-ground parts suggest that the *n*-alkane ratios that have predicted different plant groups in bog environments relatively well (e.g. Andersson et al. 2011; Bingham et al., 2010) may not be directly applicable to interpret past habitats in environments where sedges dominate and sedge roots form an important peat component. One potential way to overcome this problem could be to combine the distributions of plant group-specific *n*-alkanes, *n*-alkane ratios and sterols, if present, when analyzing the biomarker data (Ronkainen et al., 2013). The degradation of the plant matter and their chemical compounds could impede detection of especially sterols from the fen-bog transition and fen environment, where the peat **is usually** highly humified. The level of organic matter decomposition can be studied by comparing the variations in C/N ratio and the amount of total organic carbon (TOC) through the peat section (Kuhry and Vitt 1996) In addition, the ratio between 5α(H)-stanols and Δ^5-sterols can be used to infer the rate of sterol degradation because 5α(H)-stanols are known as degradation products of the Δ^5-sterols (McClymont et al., under review). A high 5α(H)-stanols and Δ^5-sterols ratio is related to anoxic conditions, shallow water table level and high rate of degradation (Bertrand et al., 2012; McClymont et al., under review). The level of degradation can also be estimated by *n*-alkane CPI value, where high CPI value is linked to high amount of well-preserved plant material (Andersson and Meyers 2012; Xie et al., 2004).

In this study we analyzed fossil plant and biomarker compositions of two peat sections. We concentrated on the fen-bog transition phase where the plant composition is known to change

(e.g. Dudová et al., 2013; Loisel and Yu, 2013; Salojärvi et al. in prep.; Tuittila et al. 2013). We aimed to investigate (1) if biomarkers can be applied to distinguish fen and bog environments, and (2) if plant-specific biomarkers can be identified from fen peat. For this we applied plant macrofossil analysis to examine the past plant compositions from the same subsamples from which the selected organic geochemical-analyses were **obtained**.

2. Material and methods

2.1. Sampling

Two peat sections (SJ5 and SJ6) were collected from two closely located peatlands in Siikajoki (64°45´N, 24°42´E) located near west coast of Gulf of Bothnia, Baltic Sea in the mid-boreal bio-climate zone in Finland (Fig. 1). A chronosequence of terrestrial ecosystems from coast to inland have been created by the postglacial isostatic rising, and along the sequence peatlands alternate with sand dunes and glaciofluvial ridges (Tuittila et al., 2013). We have previously studied vegetation, microbial communities and carbon dynamics along a transect of seven mires (SJ0 to SJ6) (e.g. Leppälä et al. 2011a,b, Laine et a. 2011, Tuittila et al. 2013, Larmola et al. *in press*). In this study we concentrated on the two oldest sites of the transect, and in particular on their sediment sections where fen-bog transition occurred, from which historical plant communities had already been studied (Tuittila et al. 2013). Site SJ5 represents a peatland stage where the fen-bog transition is still partly in progress; vegetation is a mosaic of wet fen communities and drier bog communities, the average water table level is at 12 cm below moss layer surface and the basal age of the peatland is 2520 (±20) years BP. The peat core was taken from a drier surface dominated by lawn species (*S. magellanicum*). Site SJ6 is already a true bog with vegetation formed by hummock Sphagna and dwarf shrubs, average water table level 32 cm below moss surface and the basal age of 3000

years (both cores basal ages are extrapolated from known land-uplift rate). The top section of the peat core was dominated by hummock species (*S. fuscum)*, More detailed site descriptions can be found in Leppälä et al. (2011), and Tuittila et al. (2013). The sampling depth for SJ5 was 6 – 150 cm and for SJ6 0 – 100 cm. Both cores were cut into 2 cm sample slices and analyzed with a varying down-core resolution by focusing on the fen-bog transition.

2.2. Plant macrofossil analyses

Plant macrofossil sample volume was 5 cm^3. Samples were rinsed under running water using a 140-µm sieve **and no chemical treatment was needed**. Remains retained on a sieve were identified **and the percentage in volume of constitute within the total composition of the sample was visually estimated by** using a stereomicroscope **(magnification of 10x) (e.g. Speranza et al., 2000; Mauquoy et al., 2002)** If the proportion of bryophytes exceeded 10 % of the total sample volume a high power light microscope was used to identify bryophyte species and to count proportions for different bryophyte species. Also, the proportion of unidentified organic matter (UOM) from samples was estimated (cf. Väliranta et al., 2007 and references therein).

2.2. Solvent extraction

Peat samples for solvent extraction were freeze dried and ground following the same procedure in Ronkainen et al. (2013). Lipids were extracted from ca. 0.2 g of samples using repeated ultrasonication (20 min) with 6 ml CH_2Cl_2/MeOH (3:1, v/v). Samples were saponified with 0.5 M methanolic (95%) NaOH for 2 h at 70 °C and the neutral lipids were extracted using hexane. The neutral lipids were further separated into apolar and polar compounds using activated Al_2O_3 columns, eluting with hexane/CH_2Cl_2 (9:1, v/v) and

148 CH_2Cl_2/MeOH (1:2, v/v), respectively. Prior to analysis using gas chromatography (GC) and
149 GC-mass spectrometry (GC-MS)**,** the polar fractions were derivatised using
150 bis(trimethylsilyl)trifluoroacetamide (Sigma Aldrich).
151
152 *2.3. GC-MS*
153 Apolar and polar fractions were analyzed using GC-MS with a gas chromatograph equipped
154 with flame ionisation detection (GC-FID) and split/splitless injection (280 C). Separation was
155 achieved with a fused silica column (30 m x 0.25 mm i.d) coated with 0.25μm 5% phenyl
156 methyl siloxane (HP-5MS), with He as carrier gas, and the following oven temperature
157 program: 60 – 200 °C at 20 °C/min, then to 320 °C (held 35 min) at 6°C/min. The mass
158 spectrometer was operated in full scan mode (50-650 amu/s, electron voltage 70eV, source
159 temperature 230 °C). Compounds were assigned using the NIST mass spectral database and
160 comparison with published spectra (e.g. Goad and Akihisa, 1997; Killops and Frewin, 1994).
161 Quantification was achieved through comparison of integrated peak areas in the FID
162 chromatograms and those of internal standards of known concentration (5-α-cholestane for
163 apolars and 2-nonadecanone for polars). Biomarker concentrations were normalized to total
164 organic carbon (TOC) content and are presented here as concentration per g TOC, so that
165 samples with different extent of degradation become comparable (Meyers 2003; Ortiz et al.,
166 2010). Total organic C and N_2 were measured by the CHN elemental analysis, where 1-2 mg
167 dried and ground sample was combusted at 950°C with He as a carrier gas. The reduction of
168 the combustion gases **was** carried out in a separate furnace, and separated into individual
169 components on a temperature programmed desorption column and fed into a thermal
170 conductivity detector. Results were computed as concentrations of C and N_2 from the detector
171 signal.
172

173 *2.4. Statistical analysis*

174 We applied multivariate analyses to study the variation within the plant macrofossil and
175 biomarker data (triterpenoids, sterols, stanols, *n*-alcohols (C_{20}-C_{28}) and *n*-alkanes (C_{20}-C_{35})
176 (µg/g TOC), and *n*-alkane ratios**, see the supplementary data 2**). For the analyses we
177 combined macrofossil and biomarker data from both cores by depth.

178 We first quantified separately the variation in macrofossil plant species and biomarkers
179 within the peat profiles by unconstrained (indirect) gradient analysis. **For macrofossils we**
180 **used detrended correspondence analysis (DCA) where detrending was conducted by**
181 **segments. All identified macrofossils were included in the analysis, with down-weighting**
182 **of rare species. Macrofossil data was log transformed. For biomarkers we used**
183 **principal component analysis (PCA) with centered and standardized data. No exclusion**
184 **of biomarkers due low concentrations was done.** Secondly, for the biomarker data we
185 conducted redundancy analysis (RDA), a constrained (direct) gradient analysis, to test if the
186 variation in biomarkers in the peat profiles correlates with the variation in macrofossil data.
187 For the analysis we applied the sample scores along the first and second macrofossil DCA
188 axes as explanatory variables. **Similarly to PCA the biomarker data was centered and**
189 **standardized. All constrained axes were tested with unrestricted Monte Carlo**
190 **permutation (number of permutations 499).** Multivariate analyses were conducted by
191 using Canoco for Windows 4.52 (ter Braak and Smilauer, 2002). **The correlation of the ten**
192 **most significant biomarkers identified in RDA with** depth and UOM was analysed with
193 Pearson two-tailed correlation using SPSS PASW statistics 18.

194 **We applied TWINSPAN (Two Way INdicator SPecies ANalysis, Twinspan for Windows**
195 **2.3) to** define groups of macrofossils and biomarkers that share a similar abundance peak in
196 the peat profile . For the analysis we rescaled the abundances for each macrofossil and
197 biomarker from 0 to 1 by setting the highest abundance of each unit to 1 and calculating other

values as a percentage of the highest abundance of the unit. In the analysis we used five cut levels (0.0, 0.2, 0.4, 0.6 and 0.8) of abundance and two division levels, which determines the maximum level of recursive splitting for samples and for species (Hill and Šmilauer, 2005). The statistical analyses allow us to assess the relationship of the biomarkers to the macrofossil record and to determinate if macrofossils and biomarkers can separate different environmental habitats as individual or rather as combined proxies.

3. Results

3.1. Macrofossil analyses

Sub-fossil plant assemblages revealed clearly the vegetation succession from fen to bog stage (Fig. 2). Core SJ5 showed dominance of higher plants (*Menyanthes trifoliata, Scheuzeria palustris, Equisetum* sp.) in the earliest stage of the succession (150 – 100cm). In core SJ6 these plants were present but they did not dominate (100 – 80 cm). In both of the studied cores the transition from fen to bog environment is **both identified and induced** by the appearance of *Eriophorum* sp. and sedge roots followed by a distinctive occupation of *Sphagnum* mosses at the depth of 40 – 20 cm in SJ5 and 75 – 55 cm in SJ6.

The DCA for macrofossil data (cores SJ5 and SJ6 combined) sub-divided the peat samples into three different groups: fen species (SJ5 150 – 30 cm and SJ6 98 - 62 cm), lawn species (SJ5 26 – 6 cm), and hummock species (SJ6 60 – 0 cm). The first axis describing the fen-bog gradient explained **28** % (eigenvalue **0.5298**) of the variation in the data and the second axis describing the moisture gradient on bog explained **18** % (eigenvalue **0.3491**) of the variation (Fig. 3).

3.2. Biomarker analyses

3.2.1. Apolar fraction

Figures 4a and 4b show the distribution of *n*-alkanes in both peat cores (SJ5 and SJ6). In both cores, there is up-core variation in both overall *n*-alkane concentration and the chain-length of the dominant *n*-alkane. *n*-C_{27} dominated the bottom layers (150 – 36 cm) of SJ5, excluding layers 130 – 110 cm which were dominated again by *n*-C_{23} and *n*-C_{25} alkanes, while he uppermost layers (32 – 0 cm) were mainly dominated by *n*-C_{23} and *n*-C_{25} alkanes. In the deepest layers (100 – 60 cm) in core SJ6, the dominant *n*-alkane alternated between *n*-C_{23}, *n*-C_{29} and *n*-C_{31}. The middle layers (60 – 40 cm) were dominated by *n*-C_{25} whereas the uppermost layers (30 – 0 cm) of core SJ6 were dominated by the *n*-C_{31} alkane. Different *n*-alkane ratios showed changes along the depth in both cores (Fig. 5). In core SJ5 the ratios *n*-C_{23}/*n*-C_{27}, *n*-C_{23}/*n*-C_{29}, *n*-C_{31}/*n*-C_{27} and *n*-C_{31}/*n*-C_{29} showed differences along the core, separating the top and the bottom layers apart; all ratios being higher than 1 in top 25 cm. For core SJ6 several ratios were able to separate the top and bottom layers apart e.g. *n*-C_{23}/*n*-C_{25} and *n*-C_{25}/*n*-C_{23} indicated changes happening at 62 cm (Fig 5).

The distribution of the detected triterpenoids along the cores was similar for all compounds. In core SJ5 at depths 42 – 30 cm the maximum concentrations of taraxer-14-ene (ca. 60 – 720 μg/gTOC), and taraxast-20-ene (ca. 50 – 500 μg/gTOC) were recorded. Squalene was identified only in upper layers, peaking at 30 cm (30 μg/gTOC). In core SJ6 at depths 80 – 66 cm the maximum concentrations of taraxer-14-ene (260-1050 μg/gTOC) and taraxast-20-ene (500 – 1800 μg/gTOC) were recorded. Concentration of squalene was highest at 10 cm ca. 140 μg/gTOC, downcore the concentration was ca. 10 μg/gTOC (Fig 6). The highest concentrations of taraxer-14-ene and taraxast-20-ene coincided with high counts of sedge roots and UOM in the middle layers of both cores (Figures 2 and 6).

3.2.2. Polar fraction

247 The most abundant sterols found from both cores were: brassicasterol [(22*E*)-ergosta-5,22-
248 dien-3β-ol],campesterol [campest-5-en-3β-ol], stigmasterol [(24*E*)-stigmasta-5,22-dien-3β-
249 ol], and β-sitosterol [(3β)-stigmast-5-en-3-ol]. The associated stanols of these sterols were
250 also detected: campestanol [24-methyl-5α-cholestan-3β-ol], 22E-stigmastanol [(24-ethyl-5α-
251 cholest-22-3β-ol)] and 3-stigmastanol [(24-ethyl-5α-cholestan-3β-ol)]. In core SJ5 the
252 concentration of brassicasterol was highest (ca. 150 μg/gTOC) at 50 – 30 cm; below and
253 above this depth the concentration was less than 50 μg/gTOC, although concentrations
254 increased in the uppermost 6 cm (80 μg/gTOC). The concentration of campesterol was also
255 high in the uppermost 6 cm of core SJ5, reaching concentrations of ca. 2000 μg/gTOC.
256 Between 50 – 30 cm depth the concentration of campesterol was ca. 500 – 1000 μg/gTOC,
257 and elsewhere in the core the concentration was ca. 100 – 470 μg/gTOC. Stigmasterol in core
258 SJ5 had similar concentrations and pattern as campesterol, and whilst β-sitosterol also
259 followed this same pattern the concentrations were significantly higher, reaching a maximum
260 of ca. 12 000 μg/gTOC at 30 cm depth (Fig. 6).
261 In core SJ6 the concentration of brassicasterol was higher than in core SJ5, it increased
262 towards the top of the core with highest concentration at top 30 cm (200 – 500 μg/gTOC).
263 The concentration of campesterol in core SJ6 was the highest at depths 80 – 60 and 0 cm
264 (ca.1250 – 1700 μg/gTOC). Also stigmasterol peaked at 62-60 cm (1300 μg/gTOC) and at 0
265 cm (1900 μg/gTOC). The concentration of β-sitosterol was higher in core SJ6, peaking at 72
266 cm (20 000 μg/gTOC), elsewhere concentration varied between 2500 and 10 000 μg/gTOC.
267 Tocopherol-α [(2R)-2,5,7,8-Tetramethyl-2-[(4R,8R)-(4,8,12-trimethyltridecyl)]-6-chromanol]
268 was found only from the lowermost layers of core SJ6. In both cores all stanols, campestanol,
269 22E-stigmastanol and 3-stigmastanol, were identified from bottom to upwards at all layers
270 until 10 cm in SJ5 and at 40 cm in SJ6 (Fig. 6).

In core SJ5 the concentration of phytol [(3,7,11,15-tetramethylhexadec-2-en-1-ol] was highest at 50 cm depth (ca. 2500 µg/gTOC), and the overall concentration decreased towards the top layers. In core SJ6 the concentration of phytol was highest in top layers, 60 – 0 cm, ca. 400 – 1200 µg/gTOC. Before 66 cm, phytol concentration was less than 400 µg/gTOC. The *n*-alcohol distribution in both studied cores did not vary substantially. In core SJ5 *n*-C_{22}-ol dominated depths 150, 120 and 100 – 6 cm, *n*-C_{24}-ol dominated depths 140, 130 and 110 cm, and *n*-C_{28}-ol dominated depth 70 cm. In core SJ6 *n*-C_{22}-ol dominated depths 100 – 50 cm, whereas *n*-C_{24}-ol dominated the uppermost 40 cm.

3.2.3. Statistical analyses of biomarkers

The PCA for biomarkers **produced** groups**, similar to the** DCA for macrofossils. However, when the biomarker RDA was performed (Fig.7), where sample scores from macrofossil DCA were used as explanatory variables, the biomarker distribution of the two peat profiles correlated significantly with their macrofossil compositions (pseudo F = 9.2, *p*-value = 0.002). RDA resulted in three groups similar to macrofossil DCA: fens (SJ5 150 – 30 cm and SJ6 98 – 62 cm), lawn (SJ5 26 – 6 cm), and hummock (SJ6 60 – 0 cm; Fig. 3). Biomarkers whose concentrations decreased in association with the shift from fen to bog habitat were the *n*-alkanes *n*-C_{20}, *n*-C_{22}, *n*-C_{24}, *n*-C_{26}, *n*-C_{27}, *n*-C_{28} and stanols. Markers for the top layers of core SJ5 (lawn) were e.g. the *n*-alkane ratios *n*-C_{23}/*n*-C_{27} and *n*-C_{31}/*n*-C_{29}, and for the top core of SJ6 (hummock) were e.g. *n*-C_{25}, *n*-C_{29}, and *n*-C_{28}-alcohol. The ten best-fitted biomarkers from **the** RDA are shown in figure 8. In core SJ5 *n*-alkanes *n*-C_{22}, *n*-C_{24}, *n*-C_{25}, *n*-C_{26}, *n*-C_{27} correlated positively and 22E-stigmastanol negatively with depth, and only *n*-C_{25}, *n*-C_{27}, *n*-C_{29} correlated with UOM. In core SJ6 most of the *n*-alkanes correlated positively with UOM and depth, with *n*-alkane concentrations decreasing towards top layers (Fig 8).

295 The first division of the TWINSPAN separated macrofossils from the top part of core SJ5,
296 i.e. lawn species with urs- 12-ene from the rest of the samples (Table 1). The second division
297 divided the rest of the data hummock species and biomarkers: (1) *S. fuscum* and shrub leafs
298 with C_{27} *n*-alcohol, C_{34} *n*-alkane, and squalene, and (2) fen species and biomarkers: brown-
299 mosses, sedge-roots, *Equisetum* sp., *Sch. palustris* and *M. trifoliata* together with biomarkers:
300 22E-stigmastanol, *n*-C_{35} and urs- 12-ene.

301

302 *3.2.4. Degradation measures*

303 In both cores **a** high amount of UOM corresponded to the fen-bog transition zone (SJ5: 30 –
304 20 cm and SJ6: 75 – 55 cm). In these layers 20-55 % of the plant macrofossil material was
305 unidentified. In contrast, total organic carbon (TOC) showed little variation and stayed
306 around 50 % throughout both of the cores (Fig 9). There was a clear up-core increase in the
307 C/N ratio in both cores at the fen-bog transition. The most notable increase of the carbon
308 preference index (CPI; e.g. Andersson et al. 2012) of *n*-alkanes also occurred during the
309 transition. The ratio of 5α(H)-stanols/ Δ^5-sterols (Bertrand et al. 2012) decreased towards the
310 top layers in both cores and was last detected in SJ5 at 10 cm and in SJ6 at 40 cm depth.

311

312 **3. Discussion**

313 Our results suggest that, statistically, individual biomarkers predict the fossil plant species
314 composition rather poorly, in support of observations from previous studies (e.g. Andersson
315 2012; Ficken et al., 1998; Pancost et al., 2002) that recommended that biomarkers should be
316 used as a complementary proxy. When we applied the combined data i.e. biomarkers together
317 with macrofossils as explanatory variables a clear correlation between biomarkers and fossil
318 plants was detected and the biomarkers succeeded in describing three different environments:
319 bog hummocks and lawns, and fens (Fig. 7).

Previous studies have identified the high concentrations of *n*-C_{23} and *n*-C_{25} and high ratios of *n*-C_{23} to *n*-$C_{25,}$ *n*-C_{29} and *n*-$C_{31,}$ to be characteristic to hummock *Sphagnum*-species, whereas taraxer-14-ene, taraxas-20-ene, *n*-C_{31}, and the ratio of *n*-C_{31}/*n*-C_{33} to *Ericaceae*-species (e.g. Bingham et al., 2010; McClymont et al., 2008; Nichols et al., 2006; Nott et al. 2000; Pancost et al., 2002). In contrast, the study here shows that the statistically significant biomarkers for bog hummock species, *S. fuscum*, *S. angustifolium* and *Ericaceae* roots and leafs were *n*-C_{24}-ol, *n*-C_{26}-ol, *n*-C_{28}-ol, *n*-C_{25} and *n*-C_{29} (Fig 7). These compounds were particularly effective in identifying the difference between bog and fen zones (Figures 7 and 8). However, the visual comparison between the biomarker concentrations and palaeobotanical assemblages supports the previous works that **has** linked certain plant groups with certain biomarker distributions; for example in core SJ6 the uppermost layers were dominated by *n*-C_{31}, which is an indicator of *Ericaceae*-species whose macrofossils were also present. However, the triterpenoids and sterols associated with *Ericaceae*-species (e.g. Pancost, 2002) were not detected. Although *S. fuscum* dominated the whole hummock bog peat section (SJ6) the concentration of *n*-C_{25} was **exceeded** by *n*-C_{31} when descending from 0 cm to 40 cm, but the low ratio of *n*-C_{23}/*n*-C_{25} (< 1) indicate**s** a dry *Sphagnum*- dominated environment**,** as suggested by Bingham et al. (2010). In core SJ5, similar low *n*-C_{23}/*n*-C_{25} ratios were detected in layers dominated by sedge roots, which agrees with Ronkainen et al. (2013), whose data showed this ratio to correspond both with sedge below-ground parts and *Sphagnum* mosses. However, in core SJ6 the depths that were dominated by sedge roots (100 – 66 cm) have a higher *n*-C_{23}/*n*-C_{25} ratio than comparable layers in core SJ5 (100 – 40 cm) (Fig.5). These results support the conclusion of Ronkainen et al. (2013) who suggested that the application of bog biomarkers to fen environments may be complicated by the similar signatures of *Sphagnum* mosses and sedge roots.

A recent study showed that in general the most reliable proxy for *Sphagnum* mosses in peats are the *n*-alkane ratios n-C_{23}/n-C_{27} or n-C_{23}/n-C_{29} (Bush and McInerney, 2013). When studied visually rather than through the statistical analysis our results showed that SJ6 top peat layers (60 – 0 cm) dominated by *S. fuscum* were separated from the rest of the layers by low n-C_{23}/n-C_{29} ratio (< 0.5). The statistically significant ratio n-C_{23}/n-C_{27} (< 1.5) described core SJ5 top layers (36 – 0 cm) that were dominated by *S. magellanicum* and *S. papillosum*. Other statistically significant biomarkers describing the uppermost layers of the core SJ5 with lawn habitat were n-C_{31}/n-C_{27} and n-C_{31}/n-C_{29} (Fig.7 and 8). The *n*-alkanes that dominated the lawn layer with *S. magellanicum and S. papillosum* were n-C_{23}, n-C_{25} and n-$C_{31,}$ which agree with Bingham et al. (2010). Consistent with the fact that lawns are relatively wet microhabitats when compared **with** hummocks, the previously suggested n-C_{23}/n-C_{25} and n-C_{23}/n-C_{31} ratios that should describe dry bog environment (Bingham et al. 2010) did not describe the wetter lawn environment.

In both cores the fen layers beneath bog peat consisted mainly of vascular plant remains, e.g. *M. trifoliata*, *Sch. palustris*, *Equisetum* spp. and sedges. These plants are usually dominated by odd-over-even long-chain *n*-alkanes (Fig. 2) and this was at least partly shown by RDA that grouped the mid- and long-chain *n*-alkanes C_{20}, C_{21}, C_{22}, C_{24}, C_{26}, C_{27} and C_{28} as well as three stanols as fen peat biomarkers (Fig.7). Bush and McInerney (2013) stated that n-C_{29} and n-C_{31} should not be used as general proxies for grasses and woody plants, as these two compounds are highly variable and are overlapping between these groups, but that by differences in mid-chain and long-chain *n*-alkanes *Sphagnum* mosses could be separated from them. Our results partly agree with this. In both of the studied cores the macrofossil records indicated the transition zone from fen to bog stage (SJ5; 30 – 20 cm, SJ6; 75 – 55 cm) distinctively. In core SJ5, the biomarker record indicates that the fen-bog transition is

368 characterized by a shift from long-chain *n*-alkanes (C_{27}) to mid-chain *n*-alkanes (C_{23}) at depth
369 36 cm. Yet, in core SJ6 such a clear change is not visible.

370 In our study of modern fen species, we found that sterols such as lupeol [5α-lup-20(29)-en-
371 3β-ol], obtusifoliol [4α,14α-dimethyl-5α-ergosta-8,24(24^1)-dien-3β-ol] and gramisterol [4α-
372 methyl-5α-ergosta-7,24(24^1)-dien-3β-ol] showed potential to yield information about the
373 abundance of sedge roots and mosses (Ronkainen et al., 2013). Even though sedge root
374 remains and mosses were present in the studied peat, the above mentioned group-specific
375 sterols were not detected and only brassicasterol, campesterol, stigmasterol, β-sitosterol that
376 are common to most plant species were found from fossil peat material. We attribute this
377 absence of the plant-specific sterols is due to degradation of these compounds (Lehtonen and
378 Ketola 1993) given that their concentrations in fen plants was rather low (Ronkainen et al.,
379 2013), and we conclude that appearance of stanols (Fig 6) indicates degradation of organic
380 matter since deposition (cf. McClymont et al., under review). In both cores the fen-bog
381 transition and the layers below the transition were characterized by the presence of stanols
382 and it seems that especially the 5α(H)-stanols/Δ^5-sterol ratio, which is related to anoxic
383 conditions and decay of plant material (Bertrand et al., 2012; McClymont et al. under review)
384 is a strong marker for degradation, and changes in the ratio were consistent with degradation
385 measures presented here (Fig 9). Similarly to Andersson and Meyers (2012), the CPI value
386 increases up-core in both of the studied cores, indicating better preservation of organic matter
387 at the top layers and a progressive degradation down core. In both cores CPI reaches its
388 minimum right below the transition layer, almost simultaneously where the C/N ratio
389 decreases to its minimum. In both cores the amount of UOM is clearly higher at and below
390 the fen-bog transition than in the bog peat layers. Changes in the degradation measures might
391 indicate that drier periods with lower water table level triggered the fen-bog transition
392 **(Hughes and Barber, 2003; Hughes, 2000),** resulting in accelerated plant litter decay. This

interpretation would correspond to McClymont et al. (under review) results where high 5α(H)-stanols/Δ^5-sterol ratio occurred simultaneously with low water table level. Also, around the fen-bog transition layer the concentrations of sterols and triterpenoids were high in the peat, while the dominating macrofossils were sedge roots and other parts of sedges. Previous studies have stated that sterol and triterpenoid concentrations are higher in vascular plants than mosses (e.g. Pancost et al., 2002; Ronkainen et al., 2013). The results presented here support this interpretation, and suggest that these compounds originate from vascular plants. This result is potentially important because high proportions of highly decomposed organic matter hampers reliable environmental reconstructions (cf. Ficken et al., 1998), including identifying the timing of fen-bog transitions in peat cores.

Conclusions

In this study we investigated whether biomarkers can be applied to distinguish fen and bog environments, and if plant-specific biomarkers can be identified from fen peat. Not surprisingly, the palaeobotanical analyses were able to clearly separate dry bog hummocks, moist lawns and wet fen habitats apart. With the biomarkers more robust conclusions could be drawn only when the biomarkers were combined with the macrofossil data, after which a similar kind of sub-division of peatland habitats was achieved as yielded by palaeobotanical analyses. In agreement with our previous study of fen plants, we confirm that using biomarker data from highly humified fen peat layers to achieve species level information of past plant assemblages is very challenging. Although we previously showed that certain sterols could be used as indicators for some plant groups (e.g. *Sphagnum* mosses or sedge roots), these signals were not translated into the highly humified peat. However, we were able to separate bog and fen habitats apart by the changes in *n*-alkane concentrations and the *n*-alkane ratios along the cores. Moreover, the transition zone between fen and bog habitats was

418 characterized by high concentrations of sterols and triterpenoids originating from vascular
419 plants. This proxy result seems to be applicable when reconstructing dominating plant groups
420 during the highly humified peat phases, and may potentially also be used as a degradation
421 measure as related to past changes in the water table level, and the following increase in level
422 of decay as indicated here by the 5α(H)-stanols/Δ^5-sterol ratio, CPI-value, C/N ratio and high
423 UOM.

424

425 **Acknowledgements**

426 We thank J. Menegazzo and M. West for help in the laboratory. We thank the reviewers for
427 providing constructive suggestions for improving the paper. Funding from the Academy of
428 Finland (codes 131409, 218101 and 201321) and the INTIMATE program via a COST
429 STMS grant are acknowledged.

430

431 **References**

432 Andersson R (2012) Lipid biomarkers and other geochemical indicators in
433 paleoenvironmental studies of two Arctic systems, a Russian permafrost peatland and marine
434 sediments from Lomonosov Ridge. Doctoral thesis in Geochemistry, Stockholm University,
435 Sweden.

436 Andersson, RA and Meyers PA (2012) Effect of climate change on delivery and degradation
437 of lipid biomarkers in a Holocene peat sequence in the eastern European Russian arctic.
438 *Organic Geochemistry* 53: 63-72.

439 Andersson RA, Kuhry P, Meyers P, Zebühr Y, Crill P and Mörth M (2011) Impacts of
440 paleohydrological changes on n-alkane biomarker compositions of a holocene peat sequence
441 in the eastern european russian arctic. *Organic Geochemistry* 42: 1065-1075.

442 Avsejs, LA, Nott CJ, Xie S, Maddy D, Chambers FM and Evershed RP (2002) 5-*n*-
443 Alkylresorcinols as biomarkers of sedges in an ombrotrophic peat section. *Organic*
444 *Geochemistry* 33: 861-867.

445 Baas M, Pancost R, Van Geel B and Sinninghe Damsté JS (2000) A comparative study of
446 lipids in Sphagnum species. *Organic Geochemistry* 31: 535-541.

447 Barber K, Dumayne-Peaty L, Hughes P, Mauquoy D and Scaife R (1998). Replicability and
448 variability of the recent macrofossil and proxy-climate record from raised bogs: Field
449 stratigraphy and macrofossil data from Bolton fell moss and Walton moss, Cumbria,
450 England. *Journal of Quarternary Science* 13: 515-528.

451 Bertrand O, Mansuy-Huault L, Montargès-Pelletier E, Losson B, Argant J, Ruffaldi P,
452 Etienne D, Garnier E, Dezileau L, Faure P and Michels R (2012) Molecular evidence for
453 recent land use change from a swampy environment to a pond (Lorraine, France). *Organic*
454 *Geochemistry* 50:1-10.

455 Bingham EM, McClymont EL, Väliranta M, Mauquoy D, Roberts Z, Chambers FM, et al.
456 (2010) Conservative composition of n-alkane biomarkers in Sphagnum species: Implications
457 for palaeoclimate reconstruction in ombrotrophic peat bogs. *Organic Geochemistry* 41: 214-
458 220.

459 Bush R T and McInerney F A (2013) Leaf wax n-alkane distributions in and across modern
460 plants: Implications for paleoecology and chemotaxonomy. *Geochimica Et Cosmochimica*
461 *Acta* 117: 161-179.

462 Corrigan, D., Kloos, C., O'Connor, C.S., Timoney, R.F. (1973). Alkanes from four species of
463 Sphagnum moss. *Phytochemistry* 12, 213–214.

464 Dembitsky, V.M. (1993). Lipids of bryophytes. *Progress in Lipid Research* 32, 281–356.

465 Dudová L, Hájková P, Buchtová H and Opravilová V (2013) Formation, succession and
466 landscape history of Central-European summit raised bogs: A multiproxy study from the
467 Hrubý Jeseník mountains. *Holocene* 23:230-42.

468 Ficken KJ, Barber KE and Eglinton G (1998) Lipid biomarker, δ 13C and plant macrofossil
469 stratigraphy of a Scottish montane peat bog over the last two millennia. *Organic*
470 *Geochemistry* 28: 217-237.

471 Ficken, K.J., Li, B., Swain, D.L., Eglinton, G. (2000(. An n-alkane proxy for the sedimentary
472 input of submerged/floating freshwater aquatic macrophytes. *Organic Geochemistry* 31, 745–
473 749

474 **Frolking S., Roulet N.T., Tuittila E-S., Bubier, J.L, Quillet, A, Talbot, J. Richard P.J.H.**
475 **2010. A new model of Holocene peatland net primary production, decomposition, water**
476 **balance, and peat accumulation.** ***Earth System Dynamics*** **1:1-21. doi:10.5194/esd-1-1-**
477 **2010**

478 Goad LJ and Akihisa T (1997) Analysis of sterols. Blackie Academic and Professional,
479 Blackie Academic & Professional, London.

480 Hill MO and Šmilauer P (2005) WinTWINS version 2.3. Availeble at
481 http://planet.uwc.ac.za/nisl/computing/Twinspan/userguide_twinspan.pdf (accessed 12
482 September 2013).

483 Huang X, Wang C, Zhang J, Wiesenberg GLB, Zhang Z and Xie S (2011) Comparison of
484 free lipid compositions between roots and leaves of plants in the Dajiuhu Peatland, Central
485 China. *Geochemical Journal* 45: 365-373.

486 **Hughes, P.D.M. (2000) A reappraisal of the mechanisms leading to ombrotrophy in**
487 **British raised mires. *Ecology Letters* 3 (1): 7-9.**

488 **Hughes, P.D.M. and Barber, K.E. (2003) Mire development across the fen-bog**
489 **transition on the Teifi floodplain at Tregaron Bog, Ceredigion, Wales, and a**
490 **comparison with 13 other raised bogs. *Journal of Ecology* 91 (2): 253-264.**

491 Jia G, Dungait JAJ, Bingham EM, Valiranta M, Korhola A and Evershed RP (2008) Neutral
492 monosaccharides as biomarker proxies for bog-forming plants for application to
493 palaeovegetation reconstruction in ombrotrophic peat deposits. *Organic Geochemistry* 39:
494 1790-1799.

495 Killops SD and Frewin NL (1994) Triterpenoid diagenesis and cuticular preservation.
496 *Organic Geochemistry* 21: 1193-1209.

497 Kuhry P and Vitt DH (1996) Fossil carbon/nitrogen ratios as a measure of peat
498 decomposition. *Ecology* 77: 271-275.

499 Laine AM, Byrne KA, Kiely G and Tuittila E- (2007) Patterns in vegetation and CO_2
500 dynamics along a water level gradient in a lowland blanket bog. *Ecosystems* 10: 890-905.

Laine, A. Juurola, E., Hajek, T., Tuittila, E-S. 2011*Sphagnum* growth and ecophysiology during mire succession. *Oecologia* 167: 1115-1125. DOI: 10.1007/s00442-011-2039-4

Larmola T., Leppänen, S. Tuittila E-S., Aarva M., Merilä P., Fritze H. and Tiirola, M. Methanotrophy induces nitrogen fixation during peatland development. Accepted to be published in *Proceedings of the National Academy of Sciences* in November 2013.

Lehtonen K and Ketola M (1993) Solvent-extractable lipids of Sphagnum, Carex, Bryales and Carex-Bryales peats: content and compositional features vs peat humification. *Organic Geochemistry* 20: 363-380.

Leppälä M, Laine AM, Seväkivi M- and Tuittila E- (2011) Differences in CO2 dynamics between successional mire plant communities during wet and dry summers. *Journal of Vegetation Science* 22: 357-366.

Leppälä, M., Oksanen, J. and Tuittila E-S. 2011. Methane flux dynamics during mire succession. *Oecologia* 165:489–499. DOI 10.1007/s00442-010-1754-6

Levy PE, Burden A, Cooper MDA, Dinsmore KJ, Drewer J, Evans C, et al. (2012) Methane emissions from soils: Synthesis and analysis of a large UK data set. *Global Change Biology* 18: 1657-1669.

Loisel J and Yu Z (2013) Recent acceleration of carbon accumulation in a boreal peatland, south central Alaska. *Journal of Geophysical Research G: Biogeosciences*. 118:41-53.

López-Días V, Borrego T, Blanco CG, Arboleya M, López-Sáez JA and López-Merino L (2010) Biomarkers in a peat deposit in Northern Spain (Huelga de Bayas, Asturias) as proxy for climate variation. *Journal of Chromatography A* 1217: 3538-3546.

522 Matthews E (2000). Wetlands. In: Khalil MAK (eds) *Atmospheric methane. Its role in the*
523 *Global Environment.* Berlin: Springer Verlag, pp. 202-233.

524 Mauquoy D, Engelkes T, Groot MHM, Markesteijn F, Oudejans MG, Van Der Plicht J, et al.
525 (2002) High-resolution records of late-Holocene climate change and carbon accumulation in
526 two north-west European ombrotrophic peat bogs. *Palaeogeography, Palaeoclimatology,*
527 *Palaeoecology* 186: 275-310.

528 McClymont EL, Mauquoy D, Yeloff D, Broekens P, Van Geel B, Charman DJ, et al. (2008)
529 The disappearance of Sphagnum imbricatum from Butterburn Flow, UK. *Holocene* 18: 991-
530 1002.

531 McClymont, E.L., Pancost, R.D., Bingham, E.M., Childs, E.V., Charman, D., Blundell, A.,
532 Chambers, F.M. and Evershed, R.P. (under review, 2013) Application of the stanol:Δ^5sterol
533 ratio as a proxy for palaeoredox conditions in mires. Submitted to *Organic Geochemistry*.

534 **Mauquoy, D., Van Geel, B., Blaauw, M. and Van der Plicht, J. (2002). Evidence from**
535 **northwest European bogs shows 'Little Ice Age' climatic changes driven by variations in**
536 **solar activity. *Holocene* 12 : 1-6.**

537 Meyers PA (2003) Applications of organic geochemistry to paleolimnological
538 reconstructions: A summary of examples from the Laurentian Great Lakes. *Organic*
539 *Geochemistry* 34: 261-289.

540 Moore TR, Bubier JL and Bledzki L (2007) Litter decomposition in temperate peatland
541 ecosystems: The effect of substrate and site. *Ecosystems* 10: 949-963.

542 Nichols JE, Booth RK, Jackson ST, Pendall EG and Huang Y (2006) Paleohydrologic
543 reconstruction based on n-alkane distributions in ombrotrophic peat. *Organic Geochemistry*
544 37: 1505-1513.

545 Nissinen, R. and Sewón, P. (1994). Hydrocarbons of Polytrichum commune. *Phytochemistry*
546 37, 179–182.

547 Nott CJ, Xie S, Avsejs LA, Maddy D, Chambers FM, and Evershed RP (2000) *n*-Alkane
548 distributions in ombrotrophic mires as indicators of vegetation change related to climatic
549 variation. *Organic Geochemistry* 31: 231-235.

550 Ortiz J.E., Gallego J.L.R., Torres T., Díaz-Bautista A. Sierra C. 2010. Palaeoenvironmental
551 reconstruction of Northern Spain during the last 8000 cal yr BP based on the biomarker
552 content of the Roñanzas peat bog (Asturias). Organic Geochemistry 41: 454-466.

553 Ortiz JE, Díaz-Bautista A, Aldasoro JJ, Torres T, Gallego JLR, Moreno L, et al. (2011) *n*-
554 Alkan-2-ones in peat-forming plants from the Roñanzas ombrotrophic bog (Asturias,
555 northern Spain). *Organic Geochemistry* 42: 586-592.

556 Pancost RD, Baas M, Van Geel B and Sinninghe Damsté JS (2002) Biomarkers as proxies for
557 plant inputs to peats: An example from a sub-boreal ombrotrophic bog. *Organic*
558 *Geochemistry* 33: 675-690.

559 Riutta T, Laine J, Aurela M, Rinne J, Vesala T, Laurila T, et al. (2007) Spatial variation in
560 plant community functions regulates carbon gas dynamics in a boreal fen ecosystem. *Tellus,*
561 *Series B: Chemical and Physical Meteorology* 59): 838-852.

562 Ronkainen T, McClymont EL, Väliranta M, Tuittila E-T (2013) The *n*-alkane and sterol
563 composition of living fen plants as a potential tool for palaeoecological studies. *Organic*
564 *Geochemistry* 59: 1-9.

565 Rydin H, Jeglum JK and Hooijer A (2006) *The Biology of Peatlands.* Oxford: Oxford
566 University Press.

567 Salasoo, I. (1987). Epicuticular wax alkanes of some heath plants in central Alaska.
568 *Biochemical Systematics and Ecology* 15, 105–107.

569 Sachse, D., Radke, J., Gleixner, G. (2006). DD values of individual n-alkanes from terrestrial
570 plants along a climatic gradient – implications for the sedimentary biomarker record. *Organic*
571 *Geochemistry* 37, 469–483.

572 **Speranza, A., Van Der Plicht, J.and Van Geel, B. (2000) Improving the time control of**
573 **the Subboreal/Subatlantic transition in a Czech peat sequence by 14C wiggle-matching.**
574 ***Quaternary Science Reviews* 19: 1589-1604.**

575 ter Braak CJFP and Šmilauer P (2002) CANOCO reference manual and CanoDraw for
576 Windows user's guide: Software for canonical community ordination (version 4.5). NY,
577 Ithaca: Microcomputer Power.

578 Tuittila E-S, Väliranta M, Laine A and Korhola A (2007) Controls of mire vegetation
579 succession in a southern boreal bog. *Journal of Vegetation Science* 18: 891-902.

580 Tuittila E-S, Juutinen S, Frolking S, Väliranta, M, Miettinen A, Laine A, Quillet A and Merilä
581 P (2013) Wetland chronosequence as a model of peatland development: Vegetation
582 succession, peat and carbon accumulation. *Holocene* 23: 25-35.

583 Turunen J, Tomppo E, Tolonen K, et al. (2002) Estimating carbon accumulation rates of
584 undrained mires in Finland: application to boreal and subarctic regions. The Holocene 12: 69-
585 80.

586 Wheeler BD and Proctor MCF (2000) Ecological gradients, subdivisions and terminology of
587 north-west European mires. *Journal of Ecology* 88: 187-203.

588 Vonk JE and Gustafsson O (2009) Calibrating n-alkane Sphagnum proxies in sub-Arctic
589 Scandinavia. *Organic Geochemistry* 40: 1085-1090.

590 Väliranta M, Korhola A, Seppä H, Tuittila E-, Sarmaja-Korjonen K, Laine J, et al. (2007)
591 High-resolution reconstruction of wetness dynamics in a southern boreal raised bog, Finland,
592 during the late Holocene: A quantitative approach. *Holocene* 17: 1093-1107.

593 Yu Z, Loisel J, Turetsky MR, Cai S, Zhao Y, Frolking S, et al. (2013) Evidence for elevated
594 emissions from high-latitude wetlands contributing to high atmospheric CH4 concentration in
595 the early Holocene. *Global Biogeochem Cycles* 27:131-40.

596 Yu Z, Loisel J, Brosseau DP, Beilman,DW and Hunt SJ (2010) Global peatland dynamics
597 since the Last Glacial Maximum. *Geophysical Research Letters* 37: L13402.

598 Xie S, Nott CJ, Avsejs LA, Volders F, Maddy D, Chambers FM, et al. (2000) Palaeoclimate
599 records in compound-specific δD values of a lipid biomarker in ombrotrophic peat. *Organic*
600 *Geochemistry* 31: 1053-1057.

601 Xie S, Nott CJ, Avsejs LA, Maddy D, Chambers FM and Evershed RP (2004) Molecular and
602 isotopic stratigraphy in an ombrotrophic mire for paleoclimate reconstruction. *Geochimica et*
603 *Cosmochimica Acta* 68: 2849-2862.

Zech, M., Andreev, A., Zech, R., Müller, S., Hambach, U., Frechen, M., Zech, W. (2010). Quaternary vegetation changes derived from a loess-like permafrost palaeosol sequence in northeast Siberia using alkane biomarker and pollen analyses. *Boreas* 39, 540–550.

Økland RH, Okland T and Rydgren K (2001) A Scandinavian perspective on ecological gradients in north-west European mires: Reply to Wheeler and Proctor. *Journal of Ecology 89*: 481-486.

Table caption:

Table 1. Macrofossil and biomarker communities in peat cores SJ5 and SJ6 derived from TWINSPAN (n=72, macrofossils and biomarkers in the data). Five cut levels and two divisions were used.

Supplementary data table 1. File includes published distributions of biomarkers in plants mentioned in the study.

Supplementary data table 2. File includes all the biomarker data used in the analysis.

Fig.1. Location of the study site. Samples were collected from two closely situated peatlands from the Siikajoki commune ((64°45´N, 24°42´E), Finland, Northern-Europe.
86x93mm (600 x 600 DPI)

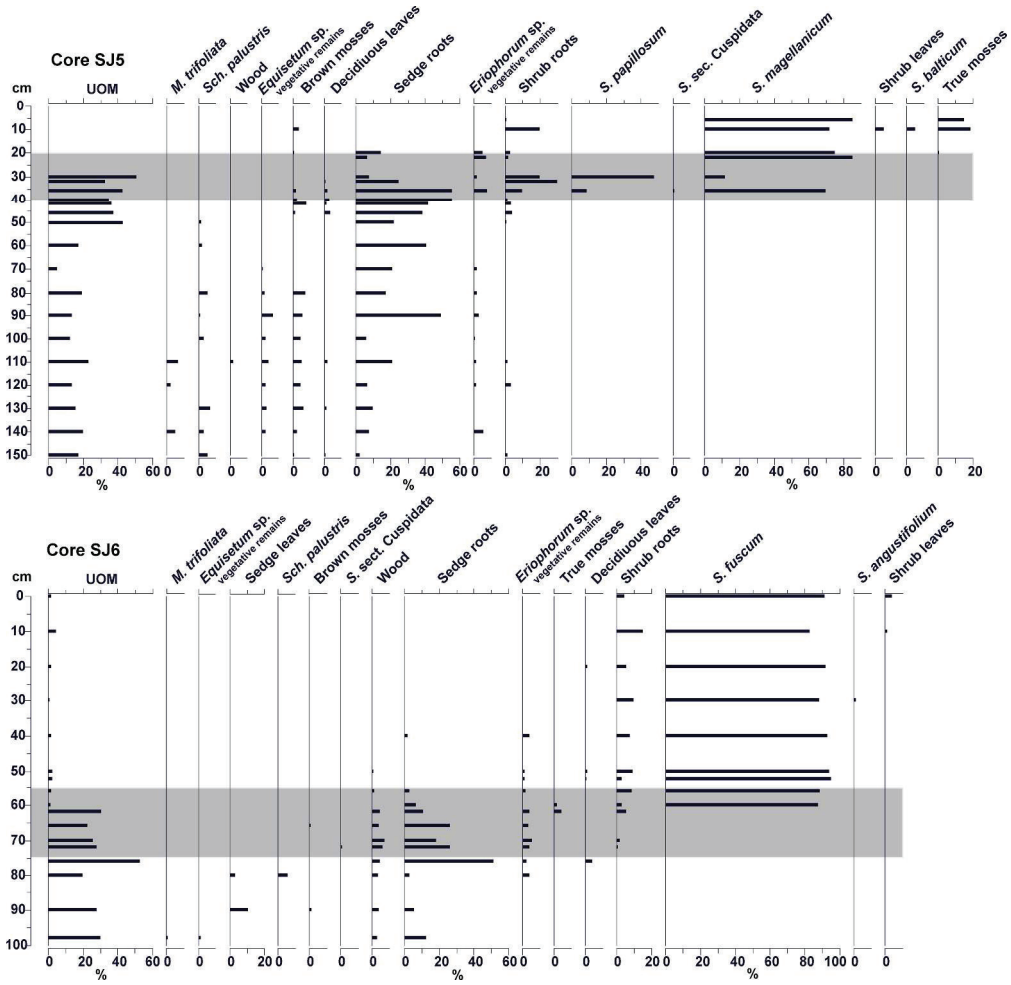

Fig. 2. Plant macrofossil records of cores SJ5 and SJ6. Macrofossil abundances are expressed as proportions (%). The fen-bog transition zone is marked with gray bar.
200x195mm (600 x 600 DPI)

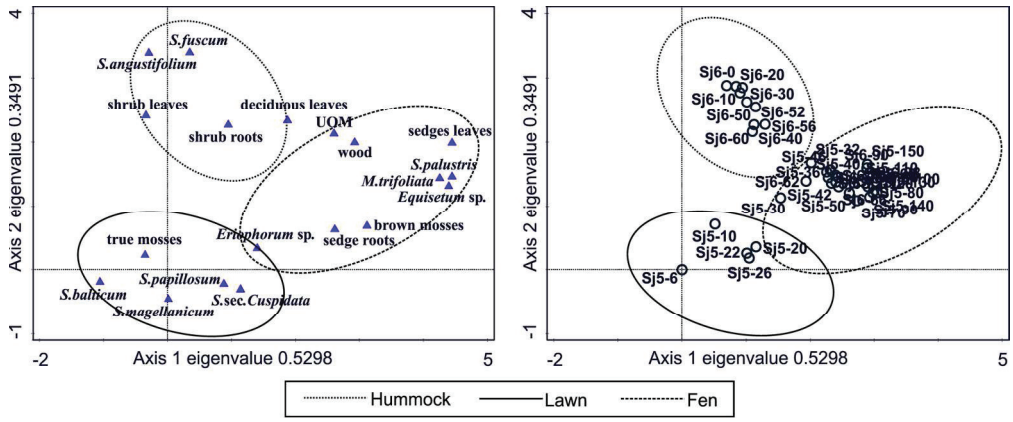

Fig. 3. DCA results of the macrofossil data of cores SJ5 and SJ6. The first axis explains 28 % (eigenvalue 0.5298) and the second axis 18 % (eigenvalue 0.3491) of the variation in the macrofossil data. Species representing hummock, lawn and fen habitats are circulated.
81x33mm (600 x 600 DPI)

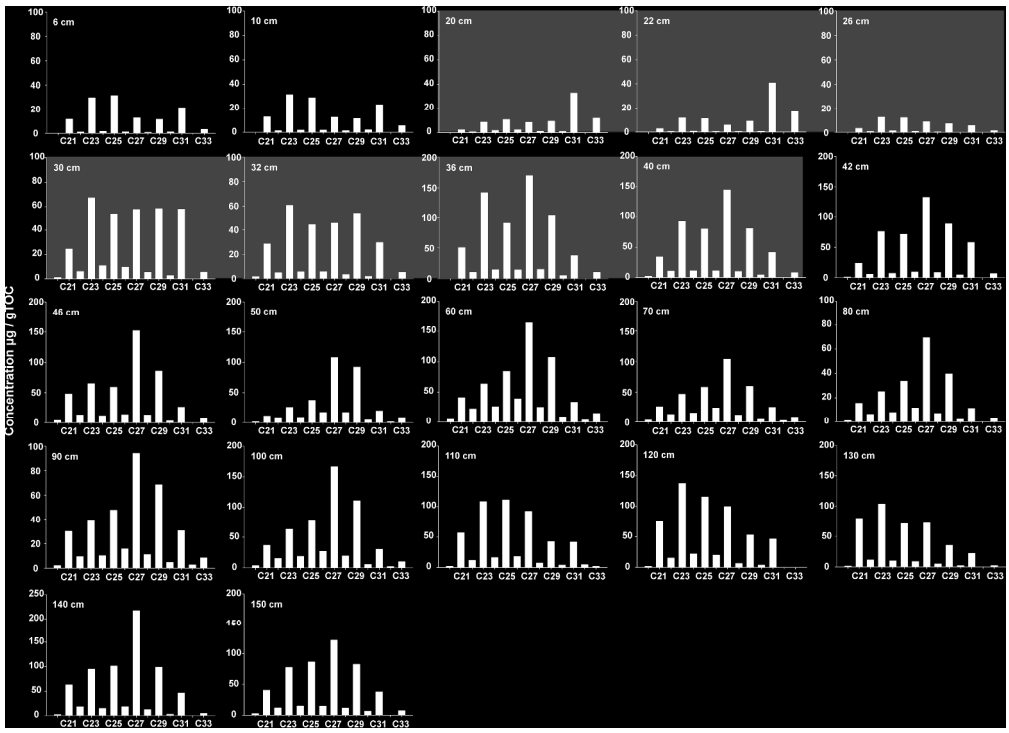

Fig. 4a. *n*-alkane concentrations (µg/gTOC) of core SJ6 by depth. The fen-bog transition zone is marked with gray.
191x137mm (600 x 600 DPI)

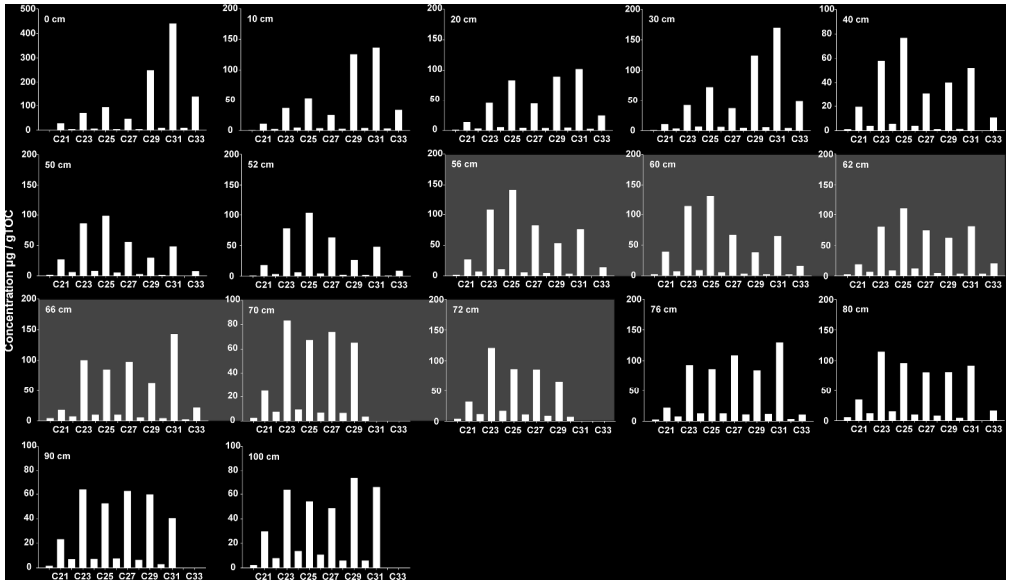

Fig. 4b. *n*-alkane concentrations (µg/gTOC) of core SJ6 by depth. The fen-bog transition zone is marked with gray.
168x96mm (600 x 600 DPI)

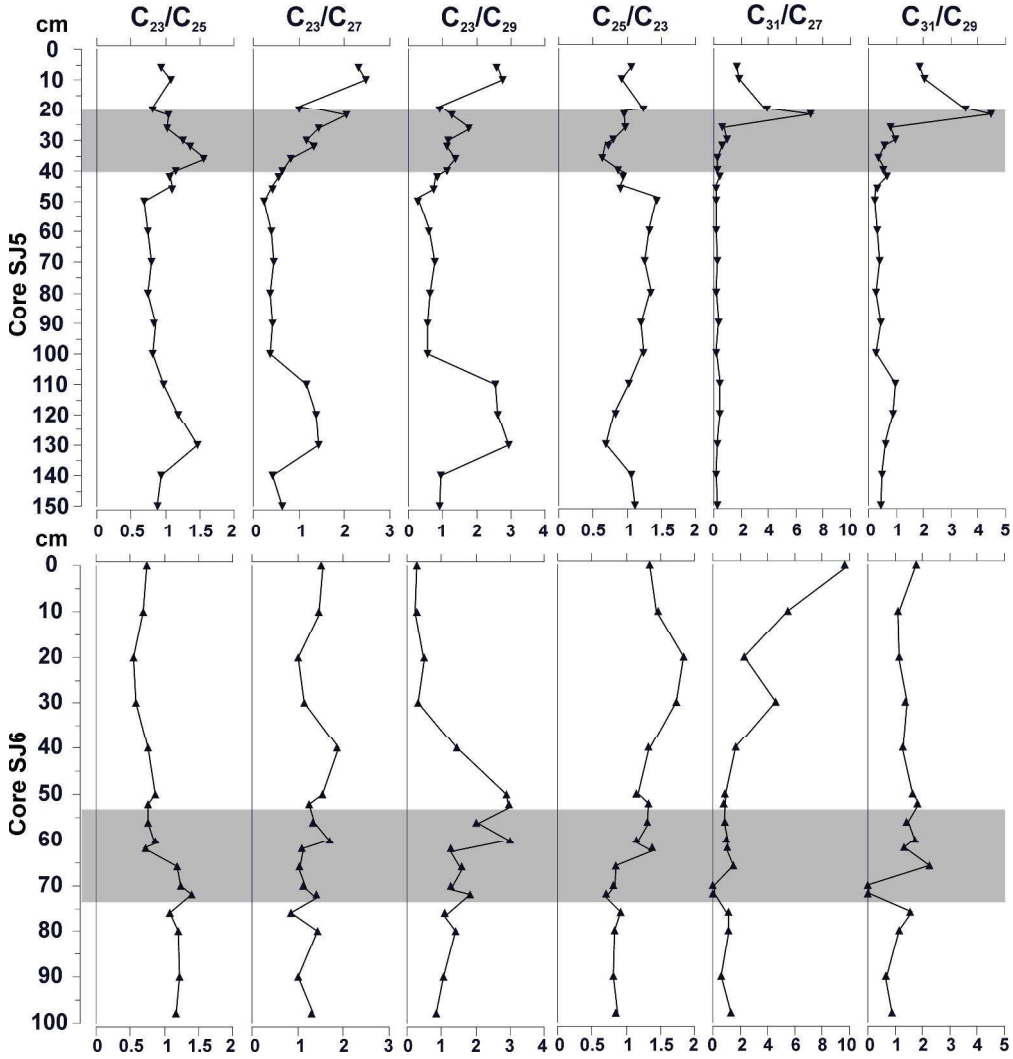

Fig. 5. *n*-alkane ratios of cores SJ5 and SJ6. The fen-bog transition zone is marked with gray bar.
188x196mm (600 x 600 DPI)

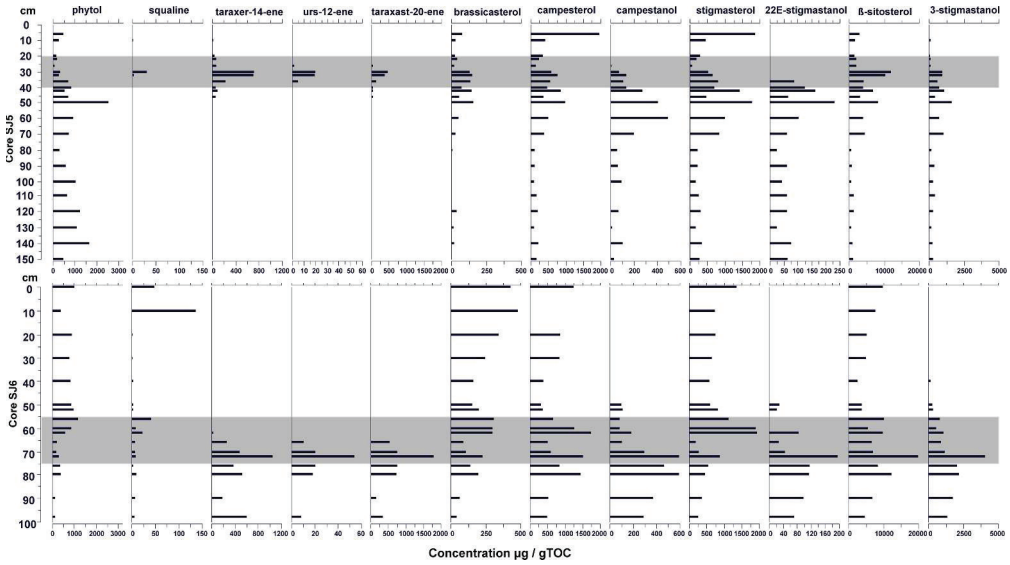

Fig. 6. Concentrations (µg/gTOC) of triterpenoids, Δ^5-sterols and 5α(H)-stanols in cores SJ5 and SJ6. The fen-bog transition zone is marked with gray bar.
161x89mm (600 x 600 DPI)

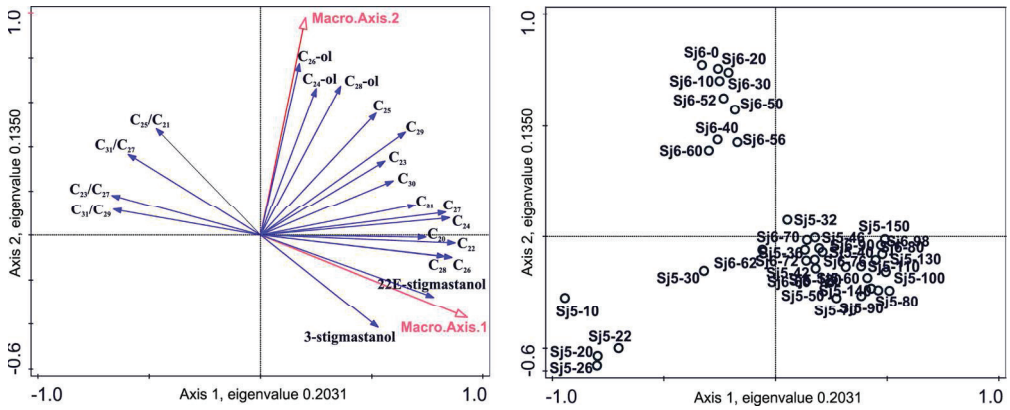

Fig. 7. RDA of biomarker data of cores SJ5 and SJ6, case scores Macro.axis.1 and Macro.axis.2 from macrofossil DCA as explanatory variables. The first axis explains 20 % (eigenvalue 0.2031) and the second axis 13 % (eigenvalue 0.1350) of the variation in the biomarker data (pseudo F = 9.2 and *p*-value = 0.002). In the figure 20 (out of 54) best fitted biomarkers are presented.
76x30mm (600 x 600 DPI)

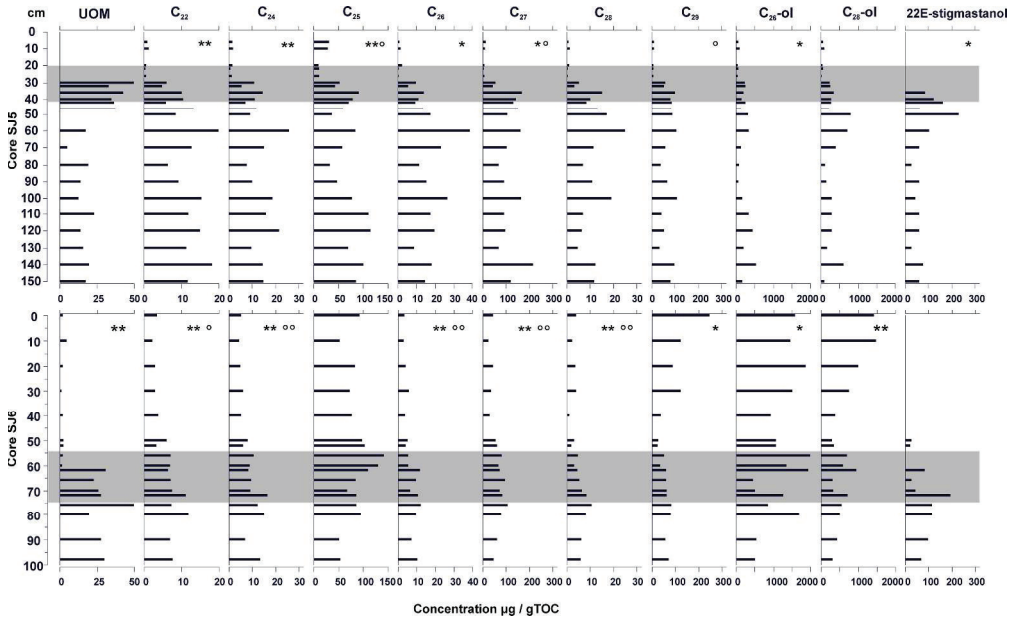

Fig. 8. Concentrations (µg/gTOC) of 10 best fitted biomarkers from biomarker RDA in cores SJ5 and SJ6. Compounds correlating with depth (sig. 0.05=*, sig. 0.01=**) and UOM (sig. 0.05=°, sig 0.01=°°) are marked. The fen-bog transition zone in both cores is marked with gray.
173x105mm (600 x 600 DPI)

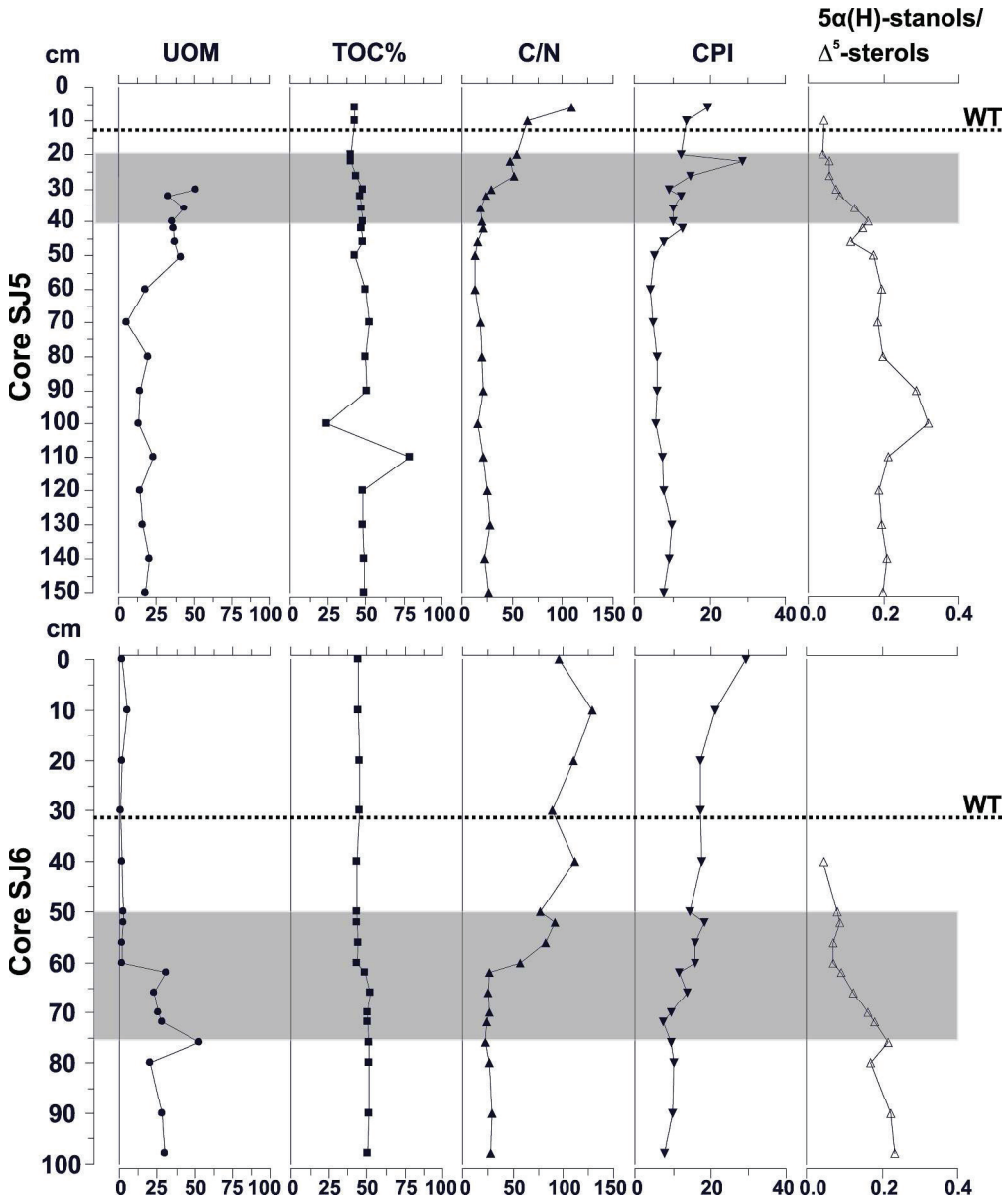

Fig. 9. Degradation measures in cores SJ5 and SJ6. UOM and TOC are presented as %, C/N ratio, CPI-value (= CPI_{alk}=((C_{21}-C_{31})+(C_{23}-C_{33})odd/2*(C_{22}-C_{32})even) according to Andersson and Mayers, 2012) and the 5α(H)-stanols/Δ^5-sterol ratio (=(campestanol+22E-stigmastanol+3-stigmastanol)/(campesterol+campestanol+stigmasterol+ 22E-stigmastanol+β-sitosterol+3-stigmastanol)) according to McClymony et al., 2013) The fen-bog transition zone is marked with gray bar and water table level (WT) with dashed line.
169x201mm (600 x 600 DPI)

First division	Second division
Hummock-fen *n* = 33 *S. fuscum, Equisetum* sp., *Sch. palustris* , wood, deciduous leaves, UOM campestanol, C_{20}-ol 22E-stigmastanol C_{27}, C_{20}, C_{32}	**Hummock *n* = 9** *S. fuscum,* shrub leaves C_{27}- ol, C_{34}, squaline **Fen *n* = 24** brown mosses, sedge roots *Equisetum* sp.*, Sch. palustris* *M. trifoliata* , campestanol, 22E-stigmastanol, urs-20-ene
Lawn *n* = 6 *S. magellanicum, S. papillosum* *S. balticum* , *S.* sect. Cuspidata true-mosses, urs-20-ene	

Table 1

Plant	Major homologue associated to plant	Studied plant species
S. fuscum	*n*-C_{25} [c, b, i, k, m]	
S. angustifolium	*n*-C_{23} [l]	
S. magellanicum	*n*-C_{25} [l]	
S. papillosum	*n*-C_{23} [l], *n*-C_{25} [l]	
S. balticum	*n*-C_{23} [l, m]	
S. sec.*Cuspidata*	*n*-C_{23} [m, o]	*S. balticum* [m], *S. lindbergii* [m], S. angustifolium [l], *S. cuspidatum* [l], *S. maju* s [l], *S. tenellum* [l], *S. riparium* [o]
True mosses	*n* -C_{27} [h], *n* -C_{31} [e, m]	*Polytrichum* sp. [e, h], *Dicranum elongatum* [m]
Brown mosses	*n*-C_{25} [o], *n*-C_{27} [o]	*Warnstorfia exannulata* [o]
M. trifoliata leaves	*n* -C_{29} [o]	
M. trifoliata roots	*n*-C_{21} [o], *n*-C_{23} [o]	
Equisetum sp.	no reference	
S. palustris	no reference	
Eriophorum sp. leaves	*n*-C_{27} [o, q], *n*-C_{29} [m]	
Eriophorum sp roots	*n*-C_{27} [o, m,	
Sedge leaves	*n* -C_{27} [b, m], *n* -C_{29} [f, o] or *n* -C_{31} [f, o]	*Carex* sp. [b, f, m, o]
Sedge roots	*n* -C_{21} [o], *n*-C_{23} [m, o], *n* -C_{27} [o],	
Shrub leafs	*n* -C_{27} [d, j, q], *n* -C_{29} [b, q], *n* -C_{31} [a, q]	*Ledum* sp. [a, m], *V. vitis-idaea* [b], *B. nana* [d ,j, m], *E. nigrum* [m], *V. uliginossum* [m], several species [q]
Shrub root	*n* -C_{27} [m], *n* -C_{29} [m], *n* -C_{31} [n]	*Eriacaceae* [n], *Betula nana* [n, m], *L. palustris* [m], *E. nigrum* [m], *V. uliginossum* [m]
Wood	*n* -C_{27} [m]	*Betula* (tree)[m]
Deciduous leaves	*n* -C_{27} [m, q], *n* -C_{29} [m, q]	*Betula* (tree)[m], several species [q]
Conifer needles	*n* -C_{27} [q], *n* -C_{29} [q], *n* -C_{31} [q]	several species [q]

[a] (Salasoo, 1987); [b] (Ficken et al., 1998); [c] (Corrigan et al., 1973); [d] (Sachse et al., 2006); [e] (Nott et al., 2000); [f] (Ficken et al., 2000); [g] (Baas et al., 2000); [h] (Nissinen and Sewón, 1994); [i] (Vonk and Gustafsson, 2009); [j] (Zech et al., 2010); [k] (Dembitsky, 1993); [l] (Bingham et al., 2010); [m] (Ronkainen et al. submitted); [n] (Andersson et al., 2011); [o] (Ronkainen et al. 2013); [q] (Tarasov et al., 2013)

n-alkanes

Sample	C20	C21	C22	C23	C24	C25	C26	C27	C28	C29	C30	C31	C32	C33	C34	C35
SJ5: 6	-	11.5	1.1	29.6	1.7	31.5	1.2	12.8	0.8	11.4	1.2	21.4	-	3.3	-	-
SJ5: 10	-	12.9	1.4	31.5	1.9	29.0	1.9	12.7	1.5	11.4	2.2	23.1	-	5.5	-	-
SJ5: 20	-	2.3	0.7	8.7	1.7	10.7	2.3	8.6	1.0	9.3	0.8	33.0	-	11.9	-	-
SJ5: 22	-	3.0	0.5	11.8	0.9	11.3	0.5	5.8	0.5	9.2	0.7	41.0	-	17.1	-	-
SJ5: 26	-	3.2	0.8	12.6	1.3	12.2	0.8	8.8	0.6	7.1	-	5.8	-	1.5	-	-
SJ5: 30	1.2	24.7	6.2	67.2	11.0	53.2	9.8	57.6	5.4	58.2	2.8	57.8	-	5.7	-	-
SJ5: 32	1.7	28.6	4.9	60.8	5.6	44.3	5.7	45.5	3.4	53.2	1.8	29.6	-	5.2	-	-
SJ5: 36	-	50.8	10.3	142.0	14.7	91.0	14.2	170.2	15.2	103.3	5.0	37.7	-	10.3	-	-
SJ5: 40	2.3	33.9	10.6	92.2	11.3	80.0	11.3	145.2	10.1	80.8	4.5	41.4	-	8.1	-	0.7
SJ5: 42	1.2	24.1	6.0	76.0	7.4	71.7	9.5	133.1	8.6	88.7	4.9	58.0	-	7.1	-	-
SJ5: 46	4.2	48.0	13.3	64.9	12.0	59.1	13.8	152.1	13.3	85.7	3.3	26.4	-	6.7	-	-
SJ5: 50	1.5	11.6	8.6	26.1	9.3	37.4	17.6	108.0	17.3	92.0	4.8	20.0	1.5	9.1	-	1.4
SJ5: 60	4.9	41.0	22.3	63.5	26.1	84.4	39.0	164.1	25.2	107.1	9.2	33.4	3.9	14.9	-	1.3
SJ5: 70	3.2	25.7	12.9	46.2	15.2	57.9	23.4	103.9	11.6	59.1	4.5	24.8	2.7	8.4	-	-
SJ5: 80	1.2	15.6	6.5	25.1	7.9	33.8	11.7	69.5	7.1	39.8	2.1	11.3	-	3.2	-	-
SJ5: 90	2.2	30.0	9.3	39.4	10.2	47.7	15.7	94.3	11.0	68.6	4.6	30.5	2.8	8.3	1.0	1.6
SJ5: 100	3.7	37.0	15.5	63.2	19.0	78.4	27.1	166.7	19.4	110.8	5.6	30.5	2.3	10.3	-	1.9
SJ5: 110	2.1	56.6	11.9	108.6	16.3	111.4	17.9	92.5	7.1	42.4	3.9	41.7	4.8	1.9	-	-
SJ5: 120	1.6	74.7	15.0	137.2	21.9	115.1	20.0	99.5	6.5	52.7	3.6	46.2	-	-	-	-
SJ5: 130	1.5	79.8	11.4	103.5	10.0	70.6	8.9	72.0	4.9	35.3	1.9	22.1	-	2.4	-	-
SJ5: 140	2.0	62.5	18.2	94.6	14.8	101.0	18.5	217.3	12.4	98.6	2.9	46.2	-	4.4	-	-
SJ5: 150	2.6	40.6	11.8	77.6	15.0	86.9	14.7	122.1	11.8	82.8	6.6	37.7	-	7.4	-	-

Sample	C20	C21	C22	C23	C24	C25	C26	C27	C28	C29	C30	C31	C32	C33	C34	C35
SJ6: 0	0.6	27.8	3.5	69.4	5.3	93.4	3.7	45.8	4.1	248.6	8.5	439.9	8.8	140.2	0.8	-
SJ6: 10	0.3	10.8	2.3	36.4	4.5	53.3	3.3	24.9	2.4	125.5	3.6	136.2	3.0	33.1	-	-
SJ6: 20	1.0	13.5	2.9	45.0	5.2	83.0	4.1	44.1	3.6	89.3	4.4	101.8	2.4	24.4	0.6	-
SJ6: 30	0.5	10.3	2.9	41.7	6.2	72.4	5.8	36.5	4.0	124.0	5.3	169.7	3.9	48.0	-	-
SJ6: 40	1.1	19.5	3.9	57.9	5.5	76.7	3.9	31.1	1.1	40.1	1.4	51.9	-	10.6	-	-
SJ6: 50	1.8	26.8	6.1	85.7	8.1	98.2	5.3	55.4	3.0	29.6	1.6	48.2	-	7.4	-	-
SJ6: 52	0.7	17.8	3.3	77.6	6.2	103.0	4.2	62.7	2.1	26.1	1.6	47.6	0.9	8.6	-	-
SJ6: 56	1.8	26.8	7.1	108.0	10.7	141.5	5.7	82.1	4.7	53.2	3.2	75.7	-	13.7	-	-
SJ6: 60	2.4	39.1	7.0	113.9	9.0	130.4	5.5	66.7	3.0	38.0	2.4	64.8	1.9	15.9	-	-
SJ6: 62	2.4	18.8	6.4	79.8	8.5	109.8	11.9	74.0	4.5	61.9	3.2	80.8	3.3	20.1	-	-
SJ6: 66	4.2	17.8	7.2	100.1	9.6	84.9	9.7	97.2	5.4	63.1	4.1	142.5	2.1	21.3	-	-
SJ6: 70	2.5	25.1	7.6	83.2	9.4	67.2	6.8	73.9	6.6	65.0	3.5	-	-	-	-	-
SJ6: 72	3.6	31.9	11.2	120.5	16.6	85.8	10.9	85.3	8.6	65.5	6.9	-	-	-	-	-
SJ6: 76	2.4	21.6	7.4	92.5	12.4	85.8	12.4	108.5	10.7	83.9	11.3	129.4	3.2	10.4	-	-
SJ6: 80	5.2	34.6	11.9	114.3	15.2	95.4	9.8	80.3	8.1	80.8	4.4	91.4	-	16.5	-	-
SJ6: 90	1.5	23.2	7.0	63.7	7.2	52.4	7.5	62.4	6.3	59.7	2.9	40.3	-	-	-	-
SJ6: 98	2.1	29.6	7.8	63.5	13.7	54.0	10.6	48.5	5.8	73.9	5.8	65.7	-	-	-	-

Concentrations are presented as µg gTOC

n- alkane ratios

Sample	C23/C25	C23/C27	C23/C29	C23/C31	C25/C29	C31/C27	C31/C29	C33/C31	C23/(C23+C29)
SJ5: 6	0.9	2.3	2.6	1.4	2.8	1.7	1.9	0.2	0.7
SJ5: 10	1.1	2.5	2.8	1.4	2.5	1.8	2.0	0.2	0.7
SJ5: 20	0.8	1.0	0.9	0.3	1.2	3.9	3.6	0.4	0.5
SJ5: 22	1.0	2.0	1.3	0.3	1.2	7.0	4.5	0.4	0.6
SJ5: 26	1.0	1.4	1.8	2.2	1.7	0.7	0.8	0.3	0.6
SJ5: 30	1.3	1.2	1.2	1.2	0.9	1.0	1.0	0.1	0.5
SJ5: 32	1.4	1.3	1.1	2.1	0.8	0.7	0.6	0.2	0.5
SJ5: 36	1.6	0.8	1.4	3.8	0.9	0.2	0.4	0.3	0.6
SJ5: 40	1.2	0.6	1.1	2.2	1.0	0.3	0.5	0.2	0.5
SJ5: 42	1.1	0.6	0.9	1.3	0.8	0.4	0.7	0.1	0.5
SJ5: 46	1.1	0.4	0.8	2.5	0.7	0.2	0.3	0.3	0.4
SJ5: 50	0.7	0.2	0.3	1.3	0.4	0.2	0.2	0.5	0.2
SJ5: 60	0.8	0.4	0.6	1.9	0.8	0.2	0.3	0.4	0.4
SJ5: 70	0.8	0.4	0.8	1.9	1.0	0.2	0.4	0.3	0.4
SJ5: 80	0.7	0.4	0.6	2.2	0.8	0.2	0.3	0.3	0.4
SJ5: 90	0.8	0.4	0.6	1.3	0.7	0.3	0.4	0.3	0.4
SJ5: 100	0.8	0.4	0.6	2.1	0.7	0.2	0.3	0.3	0.4
SJ5: 110	1.0	1.2	2.6	2.6	2.6	0.5	1.0	0.0	0.7
SJ5: 120	1.2	1.4	2.6	3.0	2.2	0.5	0.9	0.0	0.7
SJ5: 130	1.5	1.4	2.9	4.7	2.0	0.3	0.6	0.1	0.7
SJ5: 140	0.9	0.4	1.0	2.0	1.0	0.2	0.5	0.1	0.5
SJ5: 150	0.9	0.6	0.9	2.1	1.0	0.3	0.5	0.2	0.5

Sample	C23/C25	C23/C27	C23/C29	C23/C31	C25/C29	C31/C27	C31/C29	C33/C31	C23/(C23+C29)
SJ6: 0	0.7	1.5	0.3	0.2	0.4	9.6	1.8	0.3	0.2
SJ6: 10	0.7	1.5	0.3	0.3	0.4	5.5	1.1	0.2	0.2
SJ6: 20	0.5	1.0	0.5	0.4	0.9	2.3	1.1	0.2	0.3
SJ6: 30	0.6	1.1	0.3	0.2	0.6	4.6	1.4	0.3	0.3
SJ6: 40	0.8	1.9	1.4	1.1	1.9	1.7	1.3	0.2	0.6
SJ6: 50	0.9	1.5	2.9	1.8	3.3	0.9	1.6	0.2	0.7
SJ6: 52	0.8	1.2	3.0	1.6	3.9	0.8	1.8	0.2	0.7
SJ6: 56	0.8	1.3	2.0	1.4	2.7	0.9	1.4	0.2	0.7
SJ6: 60	0.9	1.7	3.0	1.8	3.4	1.0	1.7	0.2	0.7
SJ6: 62	0.7	1.1	1.3	1.0	1.8	1.1	1.3	0.2	0.6
SJ6: 66	1.2	1.0	1.6	0.7	1.3	1.5	2.3	0.1	0.6
SJ6: 70	1.2	1.1	1.3	-	1.0	0.0	0.0	-	0.6
SJ6: 72	1.4	1.4	1.8	-	1.3	0.0	0.0	-	0.6
SJ6: 76	1.1	0.9	1.1	0.7	1.0	1.2	1.5	0.1	0.5
SJ6: 80	1.2	1.4	1.4	1.3	1.2	1.1	1.1	0.2	0.6
SJ6: 90	1.2	1.0	1.1	1.6	0.9	0.6	0.7	0.0	0.5
SJ6: 98	1.2	1.3	0.9	1.0	0.7	1.4	0.9	0.0	0.5

n- alkane ratios

Sample	C25/(C25+C29)	C23/(C27+C31)	Paq	ACL C17-C35	Pwax	C23/C21	C21/C23	C25/C21	C25/C23
SJ5: 6	1.0	0.9	0.7	26.0	0.4	2.6	0.4	2.7	1.1
SJ5: 10	0.9	0.9	0.6	26.1	0.4	2.4	0.4	2.3	0.9
SJ5: 20	0.8	0.2	0.3	28.8	0.7	3.8	0.3	4.6	1.2
SJ5: 22	1.0	0.3	0.3	29.0	0.7	4.0	0.3	3.8	1.0
SJ5: 26	0.9	0.9	0.7	26.1	0.5	3.9	0.3	3.8	1.0
SJ5: 30	0.8	0.6	0.5	26.5	0.6	2.7	0.4	2.2	0.8
SJ5: 32	0.9	0.8	0.6	26.0	0.5	2.1	0.5	1.5	0.7
SJ5: 36	0.9	0.7	0.6	25.9	0.6	2.8	0.4	1.8	0.6
SJ5: 40	0.9	0.5	0.6	26.2	0.6	2.7	0.4	2.4	0.9
SJ5: 42	0.9	0.4	0.5	26.7	0.7	3.2	0.3	3.0	0.9
SJ5: 46	0.8	0.4	0.5	26.1	0.7	1.4	0.7	1.2	0.9
SJ5: 50	0.7	0.2	0.4	27.2	0.8	2.3	0.4	3.2	1.4
SJ5: 60	0.7	0.3	0.5	26.5	0.7	1.5	0.6	2.1	1.3
SJ5: 70	0.7	0.4	0.6	26.3	0.6	1.8	0.6	2.2	1.3
SJ5: 80	0.7	0.3	0.5	26.3	0.7	1.6	0.6	2.2	1.3
SJ5: 90	0.8	0.3	0.5	26.5	0.7	1.3	0.8	1.6	1.2
SJ5: 100	0.7	0.3	0.5	26.5	0.7	1.7	0.6	2.1	1.2
SJ5: 110	0.9	0.8	0.7	25.4	0.4	1.9	0.5	2.0	1.0
SJ5: 120	0.9	0.9	0.7	25.2	0.4	1.8	0.5	1.5	0.8
SJ5: 130	0.9	1.1	0.8	24.7	0.4	1.3	0.8	0.9	0.7
SJ5: 140	0.8	0.4	0.6	26.1	0.6	1.5	0.7	1.6	1.1
SJ5: 150	0.9	0.5	0.6	26.1	0.6	1.9	0.5	2.1	1.1

Sample	C25/(C25+C29)	C23/(C27+C31)	Paq	ACL C17-C35	Pwax	C23/C21	C21/C23	C25/C21	C25/C23
SJ6: 0	0.3	0.1	0.2	29.3	1.1	2.5	0.4	3.4	1.3
SJ6: 10	0.3	0.2	0.2	28.6	1.1	3.4	0.3	4.9	1.5
SJ6: 20	0.5	0.3	0.4	27.8	0.9	3.3	0.3	6.1	1.8
SJ6: 30	0.4	0.2	0.3	28.7	1.0	4.1	0.2	7.1	1.7
SJ6: 40	0.7	0.7	0.5	26.4	0.6	3.0	0.3	3.9	1.3
SJ6: 50	0.8	0.8	0.6	25.8	0.5	3.2	0.3	3.7	1.1
SJ6: 52	0.8	0.7	0.6	26.0	0.5	4.4	0.2	5.8	1.3
SJ6: 56	0.7	0.7	0.5	26.2	0.5	4.0	0.2	5.3	1.3
SJ6: 60	0.8	0.9	0.6	25.8	0.5	2.9	0.3	3.3	1.1
SJ6: 62	0.6	0.5	0.5	26.7	0.6	4.3	0.2	5.8	1.4
SJ6: 66	0.6	0.4	0.4	27.2	0.7	5.6	0.2	4.8	0.8
SJ6: 70	0.5	1.1	0.5	25.3	0.6	3.3	0.3	2.7	0.8
SJ6: 72	0.6	1.4	0.6	25.1	0.5	3.8	0.3	2.7	0.7
SJ6: 76	0.5	0.4	0.4	27.1	0.8	4.3	0.2	4.0	0.9
SJ6: 80	0.5	0.7	0.5	26.4	0.7	3.3	0.3	2.8	0.8
SJ6: 90	0.5	0.6	0.4	26.1	0.7	2.7	0.4	2.3	0.8
SJ6: 98	0.4	0.6	0.4	26.4	0.8	2.1	0.5	1.8	0.8

Triterpenoids

Sample	squaline	taraxer-14-ene	urs-12-ene	taraxast-20-ene
SJ5: 6	-	1	-	-
SJ5: 10	2.7	18.6	-	3.3
SJ5: 20	-	37.4	-	2.1
SJ5: 22	-	78.4	-	6.7
SJ5: 26	-	69.0	2.118735599	57.6
SJ5: 30	31.6	723.1	20.2	475.0
SJ5: 32	3.4	713.9	19.8	386.8
SJ5: 36	-	229.4	5.4	145.8
SJ5: 40	-	59.2	-	50.6
SJ5: 42	-	100.4	-	47.0
SJ5: 46	-	66.9	-	46.2
SJ5: 50	-	8.9	-	-
SJ5: 60	-	5.3	-	-
SJ5: 70	-	3.6	-	1.1
SJ5: 80	-	3.8	-	-
SJ5: 90	-	4.4	-	0.9
SJ5: 100	-	7.3	-	3.3
SJ5: 110	-	-	-	-
SJ5: 120	-	-	-	-
SJ5: 130	-	-	-	-
SJ5: 140	-	-	-	-
SJ5: 150	-	-	-	-

Sample	squaline	taraxer-14-ene	urs-12-ene	taraxast-20-ene
SJ6: 0	48.2	-	-	1.8
SJ6: 10	137.3	3.1	-	-
SJ6: 20	2.5	4.1	-	-
SJ6: 30	2.4	-	-	-
SJ6: 40	3.3	-	-	-
SJ6: 50	3.6	10.3	-	9.6
SJ6: 52	3.6	8.4	-	4.7
SJ6: 56	41.5	-	-	-
SJ6: 60	9.3	2.9	-	2.6
SJ6: 62	23.1	27.1	-	24.8
SJ6: 66	7.9	263.4	10.4	546.5
SJ6: 70	8.0	484.1	20.8	767.6
SJ6: 72	8.7	1053.5	54.1	1805.1
SJ6: 76	3.8	383.7	20.6	755.0
SJ6: 80	10.0	526.6	18.7	745.1
SJ6: 90	7.9	190.5	-	166.3
SJ6: 98	6.6	602.3	20.3	57.9

Concentrations are presented as µg gTOC

	Sterols						Stanols		
Sample	phytol	α-tocopherol	brassicasterol	campesterol	stigmasterol	β-sitosterol	campestanol	22E-stigmasterol-22-en-3β-ol	3-stigmastanol
SJ5: 6	488.1	-	80.6	1959.4	1873.2	3065.0	-	-	-
SJ5: 10	287.9	-	31.5	427.1	465.2	1770.2	-	-	115.5
SJ5: 20	176.9	-	26.1	362.3	304.3	1609.8	-	-	92.4
SJ5: 22	185.6	-	42.3	243.7	189.9	2050.1	-	-	146.4
SJ5: 26	94.8	-	21.4	150.9	75.2	2035.8	11.8	-	126.2
SJ5: 30	336.3	-	134.9	596.3	539.7	12073.3	73.4	-	991.1
SJ5: 32	274.3	-	149.0	773.1	652.0	10419.6	136.6	-	959.5
SJ5: 36	718.9	-	138.1	562.1	820.9	4251.1	111.6	88.6	605.4
SJ5: 40	858.0	-	77.0	473.7	700.4	4134.5	136.3	125.3	743.1
SJ5: 42	537.6	-	146.2	874.8	1438.0	6869.6	275.3	164.1	1105.6
SJ5: 46	713.8	-	57.1	374.2	472.9	3245.9	-	65.3	462.7
SJ5: 50	2537.7	-	158.8	984.2	1779.8	8246.0	408.1	233.1	1651.2
SJ5: 60	946.6	-	54.9	507.6	1003.9	3984.2	491.2	103.4	746.4
SJ5: 70	730.6	-	30.3	382.9	840.9	4538.4	203.5	61.7	1046.4
SJ5: 80	322.6	-	7.2	124.1	229.8	751.9	56.7	27.6	187.2
SJ5: 90	606.1	-	-	130.7	226.3	948.7	66.2	61.5	394.1
SJ5: 100	1039.8	-	4.6	112.2	182.2	705.8	96.6	45.0	329.8
SJ5: 110	651.9	-	-	178.0	263.0	1407.7	-	62.7	431.8
SJ5: 120	1241.6	-	38.3	214.2	314.1	1445.4	70.1	62.7	324.7
SJ5: 130	1094.2	-	17.9	107.2	173.3	620.1	14.9	27.3	175.5
SJ5: 140	1675.5	-	23.9	222.7	352.9	1134.8	104.4	77.9	271.0
SJ5: 150	485.5	-	-	179.5	290.1	1153.2	31.1	63.5	307.1

Sample	phytol	α-tocopherol	brassicasterol	campesterol	stigmasterol	β-sitosterol	campestanol	22E-stigmasterol-22-en-3β-ol	3-stigmastanol
SJ6: 0	1031.1	-	428.7	1257.5	1363.7	9863.4	-	-	-
SJ6: 10	397.0	-	481.0	-	738.9	7705.1	-	-	-
SJ6: 20	906.8	-	343.6	862.7	753.4	5262.0	-	-	-
SJ6: 30	783.1	-	246.6	840.9	660.4	5171.0	-	-	-
SJ6: 40	839.0	-	164.4	394.8	580.2	2604.4	-	-	165.8
SJ6: 50	864.6	-	153.6	318.1	610.1	3965.4	99.0	29.5	295.2
SJ6: 52	997.1	-	204.4	375.8	838.5	3930.9	109.3	23.6	368.8
SJ6: 56	1183.2	-	309.6	675.8	1132.2	10309.6	86.3	-	851.2
SJ6: 60	881.5	-	299.2	1282.8	1911.0	5639.8	86.2	-	584.3
SJ6: 62	591.6	-	299.2	1744.0	1943.0	9975.1	186.9	85.5	1108.8
SJ6: 66	213.8	-	92.6	515.4	201.8	6789.6	107.8	28.9	914.4
SJ6: 70	208.0	-	108.9	605.6	277.9	7136.2	295.7	46.4	1198.2
SJ6: 72	299.3	-	232.2	1527.3	891.0	19970.0	596.3	196.3	4082.6
SJ6: 76	360.8	-	140.7	842.6	554.8	8407.8	466.7	116.7	2100.5
SJ6: 80	391.4	146.2	200.2	1448.1	457.6	12314.4	593.6	115.5	2204.7
SJ6: 90	146.2	205.9	67.7	529.2	375.9	6840.8	371.4	99.2	1759.6
SJ6: 98	141.9	55.7	45.0	497.6	267.0	4859.4	291.9	72.0	1360.2

Concentrations are presented as µg gTOC